Title

Zinc deficiency affects the STAT1/3 signaling pathways in part through redox-mediated mechanisms.

Authors

Supasai, S
Aimo, L
Adamo, AM
et al.

Publication Date

2017-04-01

DOI

10.1016/j.redox.2016.12.027

Peer reviewed

Redox Biology 11 (2017) 469–481

Contents lists available at ScienceDirect

Redox Biology

journal homepage: www.elsevier.com/locate/redox

Research paper

Zinc deficiency affects the STAT1/3 signaling pathways in part through redox-mediated mechanisms

S. Supasai[a,b], L. Aimo[a,b], A.M. Adamo[c], G.G. Mackenzie[a], P.I. Oteiza[a,b,*]

[a] Department of Nutrition, University of California, Davis, One Shields Avenue, Davis, CA 95616, USA
[b] Department of Environmental Toxicology, University of California, Davis, One Shields Avenue, Davis, CA 95616, USA
[c] Department of Biological Chemistry and IQUIFIB (UBA-CONICET), School of Pharmacy and Biochemistry, University of Buenos Aires, Buenos Aires, Argentina

ABSTRACT

Zinc deficiency affects the development of the central nervous system (CNS) through mechanisms only partially understood. We previously showed that zinc deficiency causes CNS oxidative stress, damaging microtubules and impairing protein nuclear shuttling. STAT1 and STAT3 transcription factors, which require nuclear import for their functions, play major roles in CNS development. Thus, we investigated whether zinc deficiency disrupts STAT1 and STAT3 signaling pathways in the developing fetal CNS, characterizing the involvement of oxidative stress and the cytoskeleton in the adverse effects. Maternal (gestation day 0–19) marginal zinc deficiency (MZD) reduced STAT1 and STAT3 tyrosine phosphorylation and their nuclear translocation in the embryonic day 19 (E19) rat brain. Similar effects were observed in zinc depleted IMR-32 neuroblastoma cells, with an associated decrease in STAT1- and STAT3-dependent gene transactivation. Zinc deficiency caused oxidative stress (increased 4-hydroxynonenal-protein adducts) in E19 brain and IMR-32 cells, which was prevented in cells by supplementation with 0.5 mM α-lipoic acid (LA). In zinc depleted IMR-32 cells, the low tyrosine phosphorylation of STAT1, but not that of STAT3, recovered upon incubation with LA. STAT1 and STAT3 nuclear transports were also restored by LA. Accordingly, chemical disruption of the cytoskeleton partially reduced STAT1 and STAT3 nuclear levels. In summary, the redox-dependent tyrosine phosphorylation, and oxidant-mediated disruption of the cytoskeleton are involved in the deleterious effects of zinc deficit on STAT1 and STAT3 activation and nuclear translocation. Therefore, disruption of the STAT1 and STAT3 signaling pathways may in part explain the deleterious effects of maternal MZD on fetal brain development.

1. Introduction

Zinc is an essential nutrient that plays many critical biological roles in all tissues, including the central nervous system (CNS) [1]. Although severe zinc deficiency is relatively rare in human populations, moderate zinc deficiency is frequent throughout the world [2]. Approximately 82% of women worldwide have been reported to have insufficient zinc intake during pregnancy, and this could reach up to a 100% in developing countries [2]. Maternal zinc deficiency is associated with poor fetal growth and alters neurobehavioral development both in humans [3–6] and in animal models [7,8]. Marginal zinc deficiency (MZD) during gestation is not teratogenic but affects brain signaling and gene expression [9,10], impacting learning, memory and behavior later in life [11–13].

Zinc deficiency affects redox-regulated signals [14] that modulate cellular processes (proliferation, survival, apoptosis, differentiation, migration) central to CNS development. In neuronal cells, zinc deficiency causes an increased oxidant production via the NMDA receptor-dependent activation of NADPH oxidase and nitric oxide synthase [15]. One major associated consequence is the oxidation of tubulin thiols leading to impaired microtubule assembly [16]. In zinc depleted rat primary neuronal cultures and human IMR-32 neuroblastoma cells we observed that activated transcription factors NF-κB and NFAT fail to translocate into the nucleus given that their transport requires functional microtubules [9,17–19]. We propose that the oxidant-mediated and zinc deficiency-induced alterations in cytoskeleton dynamics could also disrupt the signal transducers and activators of transcription STAT1 and STAT3, which also require nuclear translocation to regulate transcription.

STAT1 and STAT3 play major roles in CNS development. STAT1 and STAT3 are involved in the modulation of cell apoptosis, proliferation, survival and differentiation [20–22]. STAT1-deficient mice exhibit

* Corresponding author at: Department of Nutrition, University of California, Davis, One Shields Avenue, Davis, CA 95616, USA.
E-mail address: poteiza@ucdavis.edu (P.I. Oteiza).

http://dx.doi.org/10.1016/j.redox.2016.12.027
Received 22 November 2016; Received in revised form 3 December 2016; Accepted 26 December 2016
Available online 03 January 2017
2213-2317/

a selective signaling defect in response to interferon type I and II, causing high sensitivity to infection by microbial pathogens and viruses [23,24], disruption in neuronal connectivity and deficit in social behaviors [25]. STAT1 is expressed in different areas of the developing and adult rat CNS, and its expression increases from postnatal day 0 through adulthood [26–28]. In contrast, STAT3 is widely expressed in the CNS during development, mostly at ventricular areas, where neuronal proliferation and differentiation take place [29,30]. STAT3 knockout mice are embryonic lethal [31], stressing its critical role during development. In the CNS, STAT3 is involved in neural progenitor cell proliferation [32], migration [33] and fate decisions [34].

The JAK/STAT pathway is activated by a variety of ligands including cytokines and growth factors [35–39]. Initially, ligand-receptor binding causes dimerization of the receptor subunits. In the step of signal propagation, the cytosolic domains of the receptor subunits associate to JAK tyrosine kinases. The two proximate JAKs trans-phosphorylate each other, and subsequently phosphorylate the receptor and the substrate STATs (tyrosine-701 and tyrosine-705 for STAT1 and STAT3, respectively). STATs reside in a latent state in the cytosol, upon tyrosine phosphorylation they switch to an activated state triggering homo- or/and hetero-dimerization through interactions of their SH2 domains. This leads to STAT1 and STAT3 nuclear translocation, where they bind to specific sequences in the promoter region of target genes [40].

The potential involvement of zinc and redox mechanisms on STAT1 and STAT3 modulation, as well as the impact of zinc deficiency on STAT1 and STAT3 signalings during CNS development are unknown. Given the critical roles of STAT1 and STAT3 in the CNS, this study investigated whether zinc deficiency can affect STAT1 and STAT3 signalings in the E19 rat brain. The potential involvement of zinc deficiency-associated oxidative stress and tubulin disruption on STAT1 and STAT3 nuclear transport was characterized in IMR-32 neuroblastoma cells. We show that zinc deficiency impairs STAT1 and STAT3 signalings in part through oxidative stress-associated decreased tyrosine phosphorylation and disruption of STAT1 and STAT3 nuclear shuttling.

2. Materials and methods

2.1. Materials

IMR-32 cells were obtained from the American Type Culture Collection (Rockville, MA). Cell culture media components were obtained from Invitrogen Life Technologies (Carlbad, CA). Antibodies for STAT1, STAT3, β-actin, α-tubulin, β-tubulin and heterogeneous nuclear ribonucleoprotein A1 (hnRNP), and the oligonucleotides containing the consensus sequence for STAT1 and STAT3 were obtained from Santa Cruz Biotechnology (Santa Cruz, CA). The antibody for 4-hydroxynonenal was purchased from Abcam (Cambridge, MA). Antibodies for phosphotyrosine-701 STAT1 (pY^{701}-STAT1), phosphoserine-727 STAT1 (pS^{727}-STAT1), phosphotyrosine-705 STAT3 (pY^{705}-STAT3), and phosphoserine-727 STAT3 (pS^{727}-STAT3) were purchased from Cell Signaling Technologies (Danvers, MA). The reagents for EMSA assay were obtained from Promega (Madison, WI). Polyvinylidene difluoride (PVDF) membranes were obtained from Bio-Rad (Hercules, CA, USA). Chroma Spin-10 columns were obtained from Clontech (Mountain View, CA). Vinblastine (Vb), colchicine (Col), cytochalasin D (Cyt D), α-lipoic acid (LA) and all other reagents were of the highest quality available and were purchased from Sigma (St. Louis, MO).

2.2. Animals and animal care

All procedures were in agreement with standards for the care of laboratory animals as outlined in the NIH Guide for the Care and Use of Laboratory Animals. All procedures were administered under the auspices of the Animal Resource Services of the University of California, Davis, which is accredited by the American Association for the Accreditation of Laboratory Animal Care, and adhere to the International Guiding Principles for Biomedical Research Involving Animals.

Experimental protocols were approved before implementation by the University of California, Davis Animal Use and Care Administrative Advisory Committee, and were administered through the Office of the Campus Veterinarian.

Adult Sprague-Dawley rats (Charles River, Wilmington, MA) (200–225 g) were housed individually in suspended stainless steel cages in a temperature (22–23 °C) and photoperiod (12 h light/dark)-controlled room. An egg white protein based with adequate zinc (25 μg zinc/g) was the standard control diet [41]. Animals were fed the control diet for one week before breeding. Males and females were caged together overnight and the following morning the presence of a sperm plug confirmed a successful breeding. On gestation day 0 (approximate embryonic day 0; E0), rats (6 animals/group) were divided into two groups and fed one of the following diets until gestation day 19 (E19): a control diet ad libitum (25 μg zinc/g diet, C) or a diet containing a marginally zinc-deficient concentration (10 μg zinc/g diet, MZD). Food intake was recorded daily, and body weight was measured at 5-d intervals. On gestation day 19, dams were anesthetized with isoflurane (2 mg/kg body weight), and laparotomies were performed. The gravid uterus was removed, and fetuses were collected. Fetuses were examined for gross structural malformations and weighed. Fetal brains were excised and rinsed in ice-cold PBS, and meninges were removed before weighing.

As previously described [9], a marginally zinc deficient diet imposed from gestation day 0 through 19 did not affect food intake, maternal or fetal outcomes (Supplemental Table 1).

2.3. Cell culture and incubations

IMR-32 cells were cultured at 37 °C in complex medium (55% (v/v) DMEM high glucose, 30% (v/v) Ham F-12, 5% (v/v) α-MEM) supplemented with 10% (v/v) fetal bovine serum (FBS) and antibiotics (50 U/ml penicillin, 50 μg/ml streptomycin and 0.125 μg/ml amphotericin B).

Zinc depleted FBS was prepared as previously described [42]. The zinc depleted FBS was diluted with complex medium to a final concentration of 3 mg protein/ml to match the protein concentration of the control non-depleted media. The zinc concentration of the depleted medium was 1.5 μM (1.5Zn). An aliquot of the zinc -depleted medium was supplemented with $ZnCl_2$ to obtain a final concentration of 15 μM (15Zn). Cells were grown in the control complex medium containing 10% (v/v) non-chelated FBS until confluence, after which the medium was removed and replaced by control medium or media containing 1.5 or 15 μM zinc incubated simultaneously without or with, 0.5 μM Vb, 0.5 μM Col, 0.5 μM Cyt D or 0.5 mM LA. Cells were harvested after 24 h in the different experimental conditions.

2.4. Nuclear, cytosolic and total fractions

For the E19 brains, nuclear and cytosolic fractions were isolated as previously described [43,44], with minor modifications [19]. Total, nuclear and cytosolic fractions from IMR-32 cells (2×10^7cells) were prepared as described [19].

E19 brain tissue extracts (15 mg of tissue/100 μl of lysis buffer) and IMR-32 cell extracts were prepared in lysis buffer (50 mmol/L Tris pH 7.5, 150 mM NaCl, 2 mM EDTA, 2 mM EGTA, 50 mM NaF, 2 mM $NaVaO_4$ containing inhibitors of proteases and phosphatases and 1% (v/v) Igepal). Samples were incubated at 4 °C for 20 min and then centrifuged at 10,000×g 4 °C for 20 min. Supernatants were decanted and stored at −80 °C.

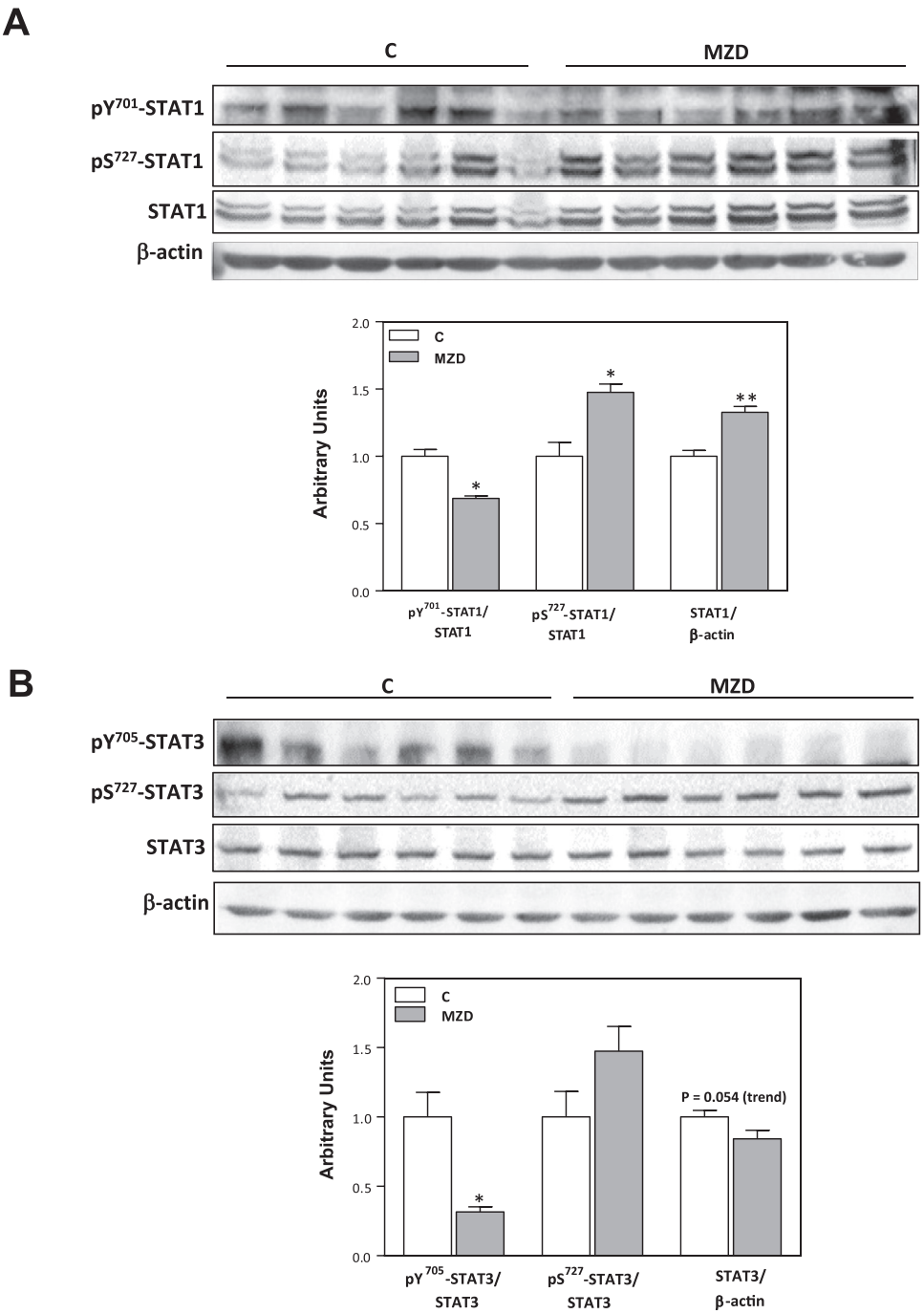

Fig. 1. Gestational MZD affects phosphorylations of STAT1 and STAT3 in E19 brain total fractions. From gestation day 0 through 19, dams were fed ad libitum control (C) or MZD diets. STAT1 and STAT3 contents and phosphorylations in E19 brain total homogenates were measured by Western blot. (A) Representative images for pY^{701}-STAT1, pS^{727}-STAT1, STAT1, and β-actin (top); and band quantifications expressed as pY^{701}-STAT1/STAT1, pS^{727}-STAT1/STAT1 and total STAT1/β-actin (bottom). (B) Representative images for pY^{705}-STAT3, pS^{727}-STAT3, STAT3, and β-actin (top), and band quantifications expressed as pY^{705}-STAT3/STAT3, pS^{727}-STAT3/STAT3 and STAT3/β-actin (bottom). Results were normalized to control values and are shown as means ± S.E.M. of 6 animals per group. *, ** Significantly different compared to C groups ($P < 0.05$ and $P < 0.01$, respectively, one-way ANOVA).

All samples were stored at −80 °C until further determinations. Protein concentration was determined [45] immediately before starting the corresponding assays.

2.5. Western blot analysis

Cell extracts containing 15–50 μg protein were diluted with 4x Laemmli sample buffer and heated for 5 min at 95 °C. Proteins were separated by 8–10% (w/v) polyacrylamide gel electrophoresis and electroblotted to PVDF membranes. Colored molecular weight (Bio-Rad, Hercules, CA) and biotinylated (Cell Signaling Technologies, Danvers, MA) standards were run simultaneously. Membranes were blocked for 1 h in 5% (w/v) nonfat milk and incubated overnight with the corresponding primary antibodies (1:1000–1:5000) in 1% (w/v) bovine albumin serum at 4 °C. After incubation with peroxidase-conjugated secondary antibodies (1:10,000–1:30,000), proteins were visualized by chemiluminescence detection in a Phosphoimager 840 (Amersham, Piscataway, NJ).

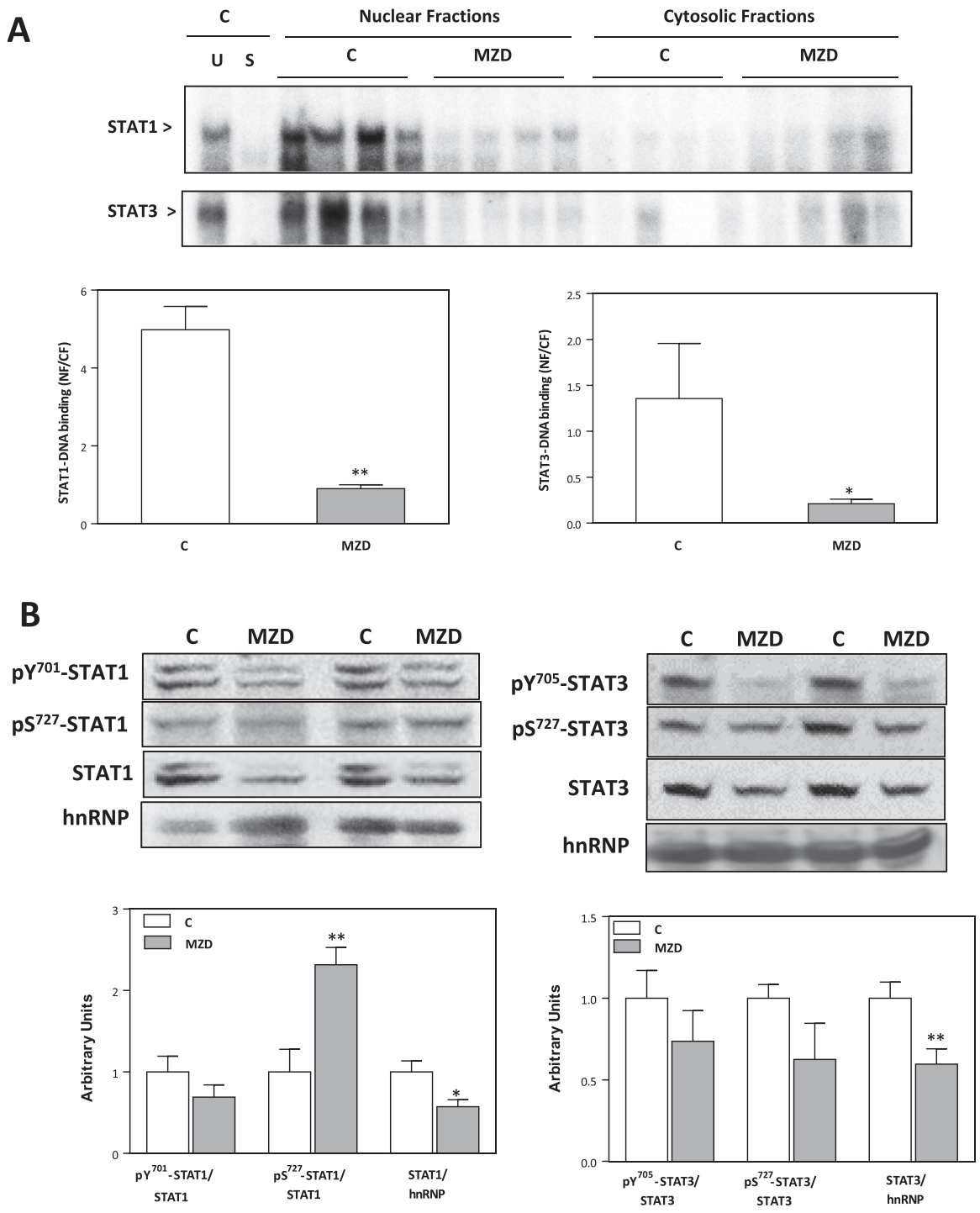

Fig. 2. Gestational MZD affects DNA binding and content of STAT1 and STAT3 in nuclear fractions isolated from E19 brains. From gestation day 0 through 19, dams were fed ad libitum control (C) or MZD diets. Nuclear and cytosolic fractions were prepared from E19 brains as described in the Materials and Methods section. (A) EMSA for STAT1 and STAT3 in nuclear and cytosolic fractions. To determine the specificity of each transcription factor-DNA complex, a control nuclear fraction was incubated in the presence of a 100-fold molar excess of unlabeled oligonucleotide containing the consensus sequence for either the specific (S) or an unspecific (U) transcription factor before the binding assay. Bands were quantified and the ratio nuclear/cytosolic DNA binding (NF/CF) was calculated. (B) Western blots for pY^{701}-STAT1, pS^{727}-STAT1, and STAT1 (left); and pY^{705}-STAT3, pS^{727}-STAT3, and STAT3 (right); and hnRNP as the nuclear housekeeping protein. After quantification, results were expressed as pY^{701}-STAT1/STAT1, pS^{727}-STAT1/STAT1 and STAT1/hnRNP (bottom left), or pY^{705}-STAT3/STAT3, pS^{727}-STAT3/STAT3, and STAT3/hnRNP (bottom right). Results were normalized to control values and are shown as means ± S.E.M. of 6 animals per group. *, ** Significantly different compared to C groups ($P < 0.05$ and $P < 0.01$, respectively, one-way ANOVA).

2.6. Electrophoretic mobility shift assay (EMSA)

Oligonucleotides containing the consensus sequence of STAT1 (5′-CAT GTT ATG CAT ATT CCT GTA AGT G-3′) or STAT3 (5′-GAT CCT TCT GGG AAT TCC TAG ATC-3′) were end-labeled with (^{32}P) ATP using T4 polynucleotide kinase and purified using Chroma Spin-10 columns. Samples were incubated with labeled oligonucleotide (20,000–30,000 cpm) for 20 min at room temperature in 1X binding buffer (5X binding buffer: 50 mM Tris-HCl buffer, pH 7.5, containing 20% (v/v) glycerol, 5 mM $MgCl_2$, 2.5 mM EDTA, 2.5 mM DTT, 250 mM NaCl and 0.25 mg/ml poly(dI-dC)). Products were separated by electrophoresis in a 6% (w/v) non-denaturing polyacrylamide gel

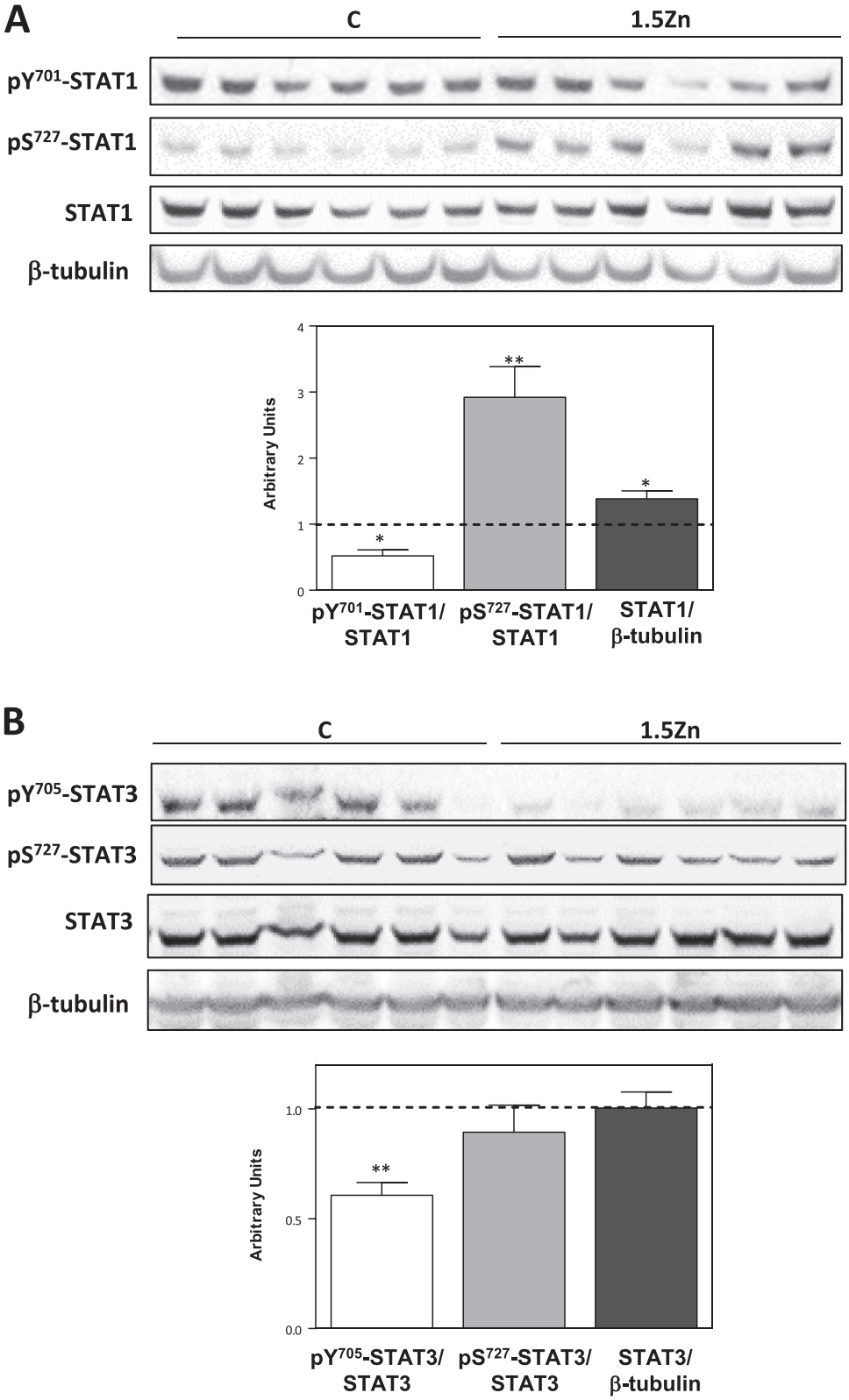

Fig. 3. Zinc deficiency affects total protein content and phosphorylation patterns of STAT1 and STAT3 in IMR-32 total fractions. Total cell fractions were isolated from IMR-32 cells incubated for 24 h in control (C) or zinc -depleted (1.5 μM zinc (1.5Zn)) medium. STAT1 and STAT3 contents and phosphorylations were measured by Western blot. (A) Representative images for pY^{701}-STAT1, pS^{727}-STAT1, STAT1, and β-tubulin as the housekeeping protein (top), and their quantification expressed as pY^{701}-STAT1/STAT1, pS^{727}-STAT1/STAT1 and STAT1/β-tubulin (bottom). (B) Representative images for pY^{705}-STAT3, pS^{727}-STAT3, STAT3, and β-tubulin (top), and their quantification expressed as pY^{705}-STAT3/STAT3, pS^{727}-STAT3/STAT3, and STAT3/β-tubulin (bottom). Results were normalized to control values (dotted lined) and shown as means ± S.E.M. of four independent experiments. *, ** Significantly different compared to C groups ($P < 0.05$ and $P < 0.01$, respectively, one-way ANOVA).

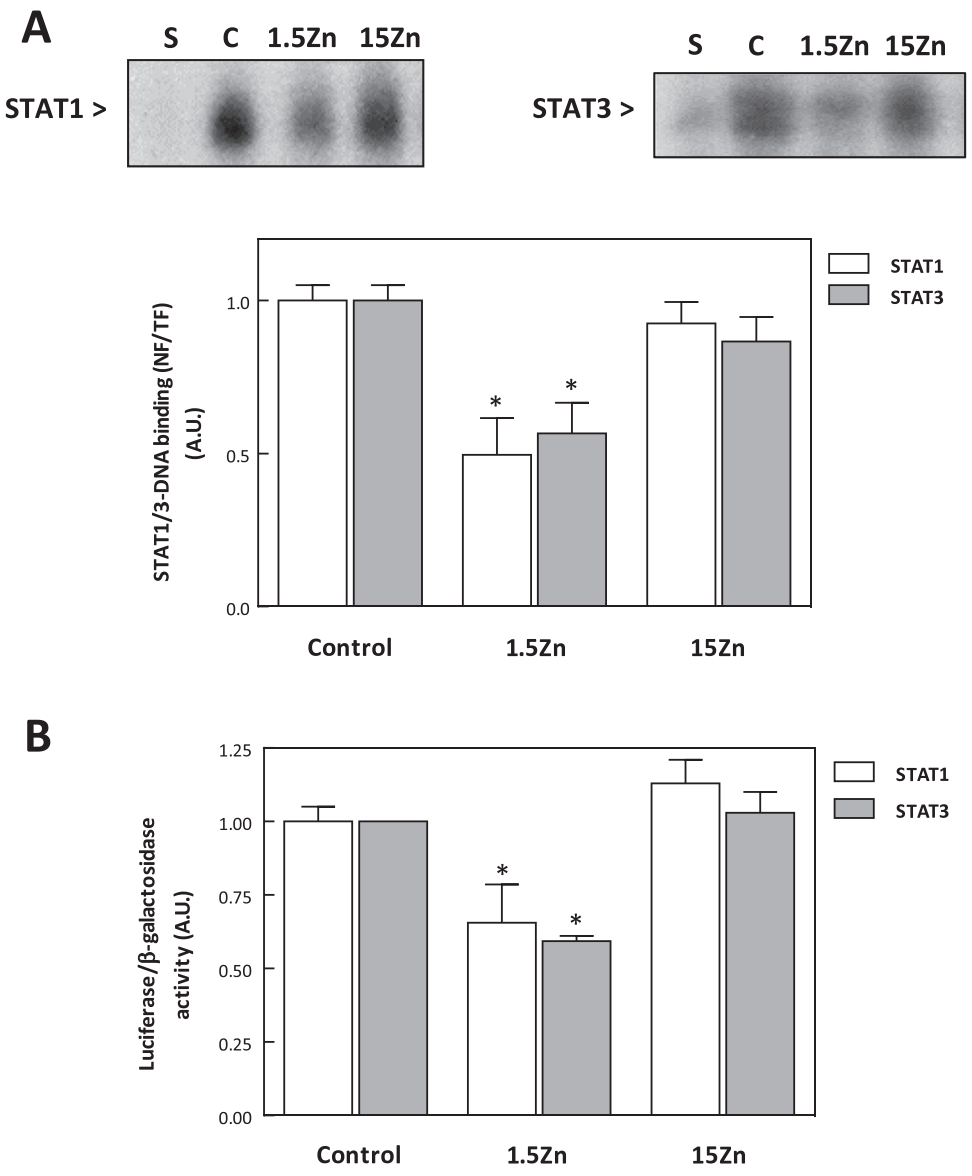

Fig. 4. Zinc deficiency affects nuclear STAT1- and STAT3-DNA binding, and transactivation of STAT1 and STAT3-dependent genes in IMR-32 cells. Nuclear and total cell fractions were isolated after incubating IMR-32 cells for 24 h in control medium (C), or in chelated medium containing 1.5 μM zinc (1.5Zn), or 15 μM zinc (15Zn). (A) Representative image of an EMSA for STAT1 and STAT3 in nuclear fractions (top). A control nuclear fraction was incubated in the presence of a 100-fold molar excess of unlabeled oligonucleotide containing the consensus sequence for aspecific (S) transcription factor before the binding assay. Bands were quantified, results expressed as the ratio nuclear/total fraction binding (NF/TF) for STAT1 (white bars) and STAT3 (grey bars), and normalized to control values. Results are shown as means ± S.E.M. of three independent experiments. (B) Transactivation of STAT1- and STAT3-driven luciferase was measured as described in Materials and Methods in cells incubated for 24 h in control, 1.5Zn or 15Zn medium. Data are expressed as the ratio luciferase activity/β-galactosidase activity. Results are shown as means ± S.E.M of three independent experiments. *Significantly different compared to the C groups ($P < 0.05$, one-way ANOVA).

using 0.5X TBE (Tris/borate 45 mM, EDTA 1 mM) as the running buffer. Gels were dried and the radioactivity quantitated in a Phosphoimager 840 (Amersham Pharmacia Biotech. Inc., Piscataway, NJ).

2.7. Transfections

IMR-32 cells were seeded in 6 well plates. After 24 h in culture, cells (2.5×10^6 cells) were transfected with Lipofect-AMINE™ 2000 according to the manufacturer's protocols (Invitrogen Life Technologies, Carlsbad, CA, USA). A vector expressing β-galactosidase (2 μg of DNA) as an internal control for transfection efficiency was co-transfected with STAT1-LUC or STAT3-LUC plasmids (1 μg of DNA). After 24 h of transfection, cells were treated with control, 1.5Zn or 15Zn media. Treated cells were harvested 24 h later and lysed. β-galactosidase and luciferase activities were determined following the manufacturer's protocol (Promega, Madison, WI).

2.8. Immunohistochemistry

The E19 brains were dissected out and fixed in 4% (w/v) paraformaldehyde in PBS (pH 7.2) overnight. Tissues were washed twice with PBS, incubated in 15% (w/v) sucrose in PBS for 24 h, and subsequently in 30% (w/v) sucrose for 3 d, after which brains were submerged in Cryoplast (Biopack, Buenos Aires, Argentina), frozen, cut into 18-μm coronal sections on a Leica CM 1850 cryotome (Leica Microsystems, Nussloch, Germany) and mounted on positively charged slides. Sections were processed for antigen retrieval by incubation in 10 mM sodium citrate buffer (pH 6.0) containing 0.05% (v/v) Tween 20 for 10 min at 95 °C, washed twice with PBS and then blocked for

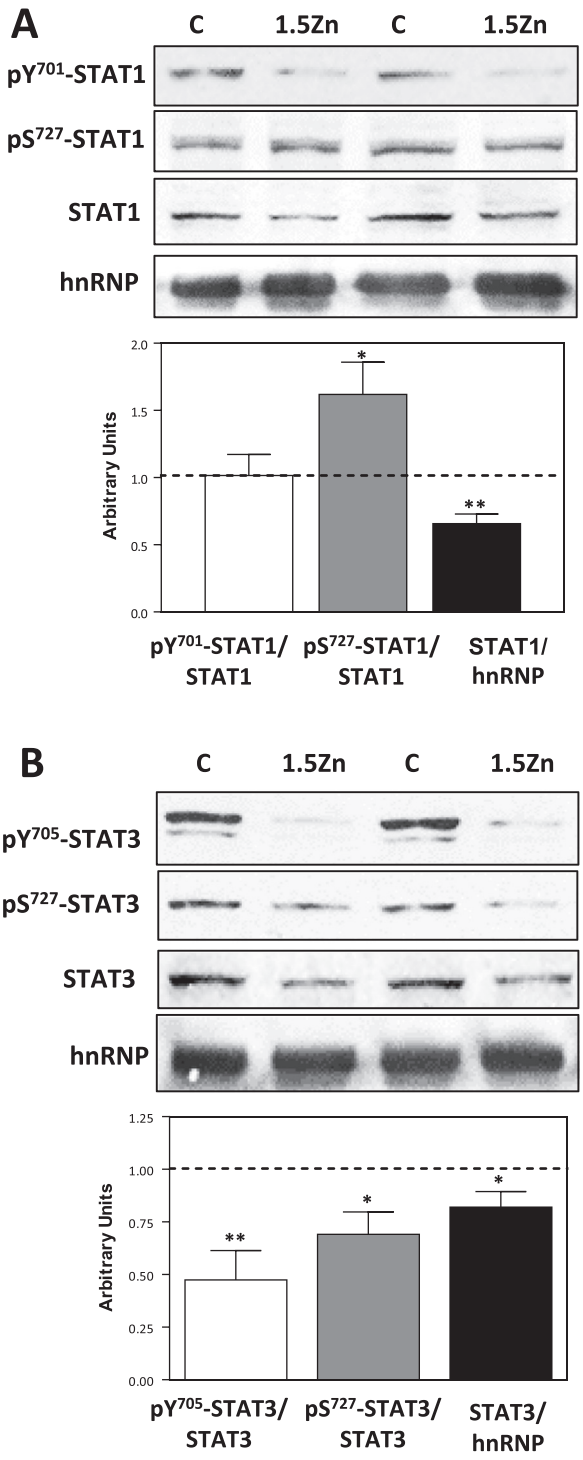

Fig. 5. Zinc deficiency affects total protein content and phosphorylation patterns of STAT1 and STAT3 in IMR-32 cell nuclear fractions. Nuclear fractions were isolated from IMR-32 cells incubated for 24 h in control (C) or 1.5Zn medium. STAT1 and STAT3 content and phosphorylations were measured by Western blot. (A) Representative images for pY^{701}-STAT1, pS^{727}-STAT1, STAT1, and hnRNP as the nuclear housekeeping protein (top), and their quantification expressed as pY^{701}-STAT1/STAT1, pS^{727}-STAT1/STAT1 and STAT1/hnRNP (bottom). (B) Representative images for pY^{705}-STAT3, pS^{727}-STAT3, STAT3, and hnRNP (top), and their quantification expressed as pY^{705}-STAT3/STAT3, pS^{727}-STAT3/STAT3, and STAT3/hnRNP (bottom). Results were normalized to control values (dotted lined) and shown as means ± S.E.M. of four independent experiments. *, ** Significantly different compared to C groups ($P < 0.05$ and $P < 0.01$, respectively, one-way ANOVA).

45 min in 1% (v/v) donkey serum, 0.1% (v/v) Triton X-100 in 0.1 M PBS and incubated overnight at 4 °C with 4-HNE (1:100) primary antibody in blocking solution. Sections were then washed with PBS and incubated for 2 h at room temperature with a biotinylated secondary antibody diluted in blocking buffer (Vector Laboratories, Burlingame, CA). To visualize the antigen–antibody complex, the secondary antibodies were labeled with avidin–horseradish peroxidase for 2 h at room temperature followed by exposure to 3,3-diaminobenzene (DAB; Vector Laboratories, Burlingame, CA) for 3 min. Slides were washed, dehydrated, and cover slips were mounted with Permount (Fischer Sci, Hampton, NH). Two sections per animal (one from each litter, n=3/group) were imaged on an Olympus BX50 epifluorescence microscope (Tokyo, Japan).

2.9. Statistical analysis

One-way analysis of variance (ANOVA) test, followed by Fisher's PLSD (protected least-squares difference) test and correlations, were performed using the routines available in Statview 5.0 (SAS Institute, Cary, NC, USA.). A p value < 0.05 was considered statistically significant. Values are given as means ± S.E.M. The litter was considered the statistical unit.

3. Results

3.1. Gestational MZD affects the modulation and nuclear translocation of STAT1 and STAT3 in the E19 brain

In the E19 brain we initially measured an early event in STAT1/3 activation, the phosphorylation of tyrosine residues (Tyr701 and 705 for STAT1 and STAT3, respectively) by Western blot **(**Fig. 1**).** STAT1 and STAT3 tyrosine phosphorylation levels were lower (31% and 68%, respectively) in MZD fetal brains compared to controls **(**Fig. 1**A and B)**. Total STAT1 content was 33% higher, while a trend (p= 0.054) for lower total STAT3 was found in MZD fetal brains compared to controls. STAT1 and STAT3 were also phosphorylated in serine residues (Ser727). In MZD E19 brains serine phosphorylation levels were 48% higher or unchanged for STAT1 and STAT3, respectively, compared to controls **(**Fig. 1**A and B)**.

We next investigated the effects of gestational MZD on STAT1 and STAT3 nuclear transport in E19 brains. Initially, STAT1- and STAT3-DNA binding was measured in E19 brain nuclear fractions by EMSA. Ratios of nuclear/cytosolic STAT1- and STAT3-DNA binding were significantly lower in MZD E19 brains than in controls (82% and 84%, respectively) (Fig. 2**A**). To further investigate if the nuclear transport of STAT1 and STAT3 could be affected by gestational MZD, we measured by Western blot the total content of STAT1 and STAT3 in nuclear fractions. The nuclear content of total STAT1 and STAT3 was lower (43% and 40%, respectively) in MZD fetal brains compared to controls **(**Fig. 2**B)**. Levels of tyrosine phosphorylation for STAT1 and STAT3 in nuclear fractions were similar in both groups. Serine phosphorylation level of STAT1 was 2.3-fold higher, while that of STAT3 was similar, in the nuclear fraction from MZD E19 brains compared to controls **(**Fig. 2**B)**. Alterations in the nuclear transport of STAT1 and STAT3 as a consequence of zinc deficiency are consistent with our previous findings for two other transcription factors, NF-κB and NFAT [9].

3.2. Zinc deficiency impairs STAT1 and STAT3 phosphorylation, DNA binding, and transactivating activity in human IMR-32 neuroblastoma cells

To further investigate the mechanisms underlying zinc deficiency-induced impaired STAT1 and STAT3 regulation, we used human IMR-32 neuroblastoma cells. In this cell line we previously showed that zinc deficit promotes increased oxidant production, causes tubulin oxidation, alters polymerization and consequently inhibits NF-κB and NFAT

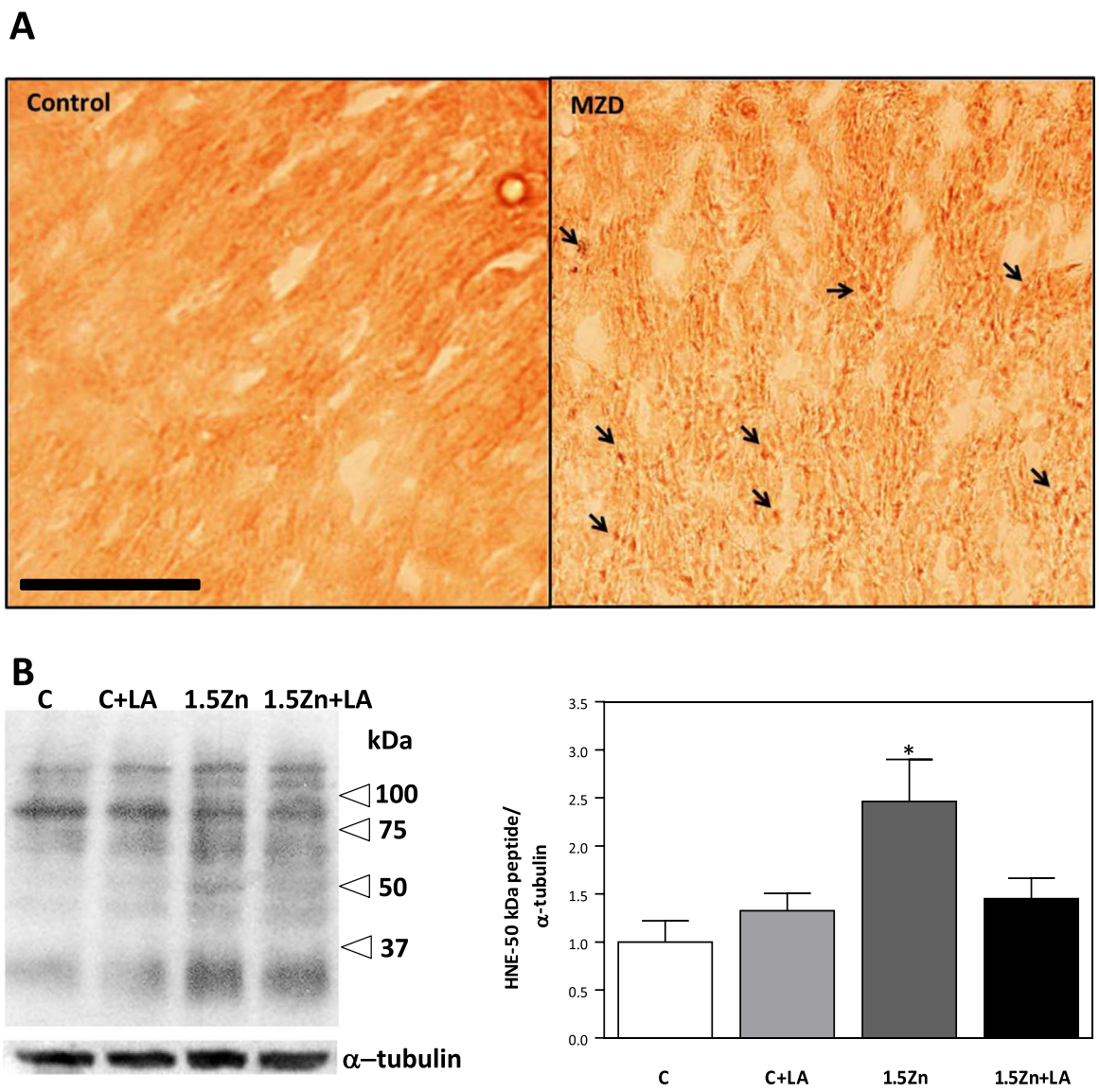

Fig. 6. Zinc deficiency causes increased levels of 4-HNE-protein adducts in E19 brain and IMR-32 cells. (A) Protein-HNE adducts in E19 brains were measured by immunohistochemistry as described in the methods section. Arrows indicate examples of HNE-protein adducts. Scale bar =20 μm. (B) Protein-HNE adducts were measured by Western blot in total cell fractions from IMR-32 cells incubated for 24 h in control (C), or zinc depleted (1.5Zn) medium with or without supplementation with 0.5 mM α-lipoic acid (LA). The band corresponding to a 50 kDa peptide was quantified. Results were normalized to control values and shown as means ± S.E.M. of three independent experiments. *Significantly different compared to C groups ($P < 0.05$, one-way ANOVA).

nuclear import [17,19]. Cells were incubated for 24 h in control, zinc-depleted (1.5Zn), or zinc-repleted (15 μM zinc, 15Zn) medium. Consistent with results in the E19 brain, STAT1 showed 48% lower and 300% higher tyrosine and serine phosphorylation, respectively, in zinc deficient compared to control cells **(**Fig. 3**A)**. Total STAT1 protein content was 39% higher in 1.5Zn than in control cells **(**Fig. 3**A)**. STAT3 tyrosine phosphorylation, was significantly lower (39%) in zinc-deficient than in control cells **(**Fig. 3**B)**. Unlike findings for STAT1, total STAT3 and serine phosphorylation levels were not affected by zinc depletion.

STAT1- and STAT3-DNA binding was measured by EMSA in total cell extracts and in nuclear fractions. The ratio nuclear/total STAT1- and STAT3-DNA binding was significantly lower (50% and 43%, respectively) in cells cultured in zinc depleted medium compared to those incubated in control or 15Zn medium **(**Fig. 4**A)**. We next measured the STAT1/3 transactivation activity using a reporter gene assay. After 24 h incubation in control, 1.5Zn or 15Zn medium, STAT1- and STAT3-driven luciferase activity (corrected for β-galactosidase activity) was 34% and 41% lower, respectively, in cells incubated in 1.5Zn medium than in control or 15Zn medium **(**Fig. 4**B)**. Consistent with the DNA binding results, STAT1- and STAT3-mediated luciferase activity was recovered by repletion of 1.5Zn medium with 15 μM zinc (15Zn).

3.3. Zinc deficiency disrupts STAT1 and STAT3 nuclear translocation and phosphorylations in IMR-32 cells

We next evaluated the effects of zinc deficiency on STAT1 and STAT3 nuclear translocation using Western blot. Total STAT1 and STAT3 nuclear content were 34% and 18% lower in zinc deficient compared to control cells **(**Fig. 5**A and B)** Similar to results for the E19 brain, in IMR-32 cells zinc deficiency did not affect nuclear STAT1 tyrosine phosphorylation but caused higher 62% serine phosphorylation levels compared to controls **(**Fig. 5**A)**. Nuclear STAT3 tyrosine- and serine-phosphorylation levels were 53% and 31% lower in nuclear fractions from zinc-deficient than in control cells **(**Fig. 5**B).**

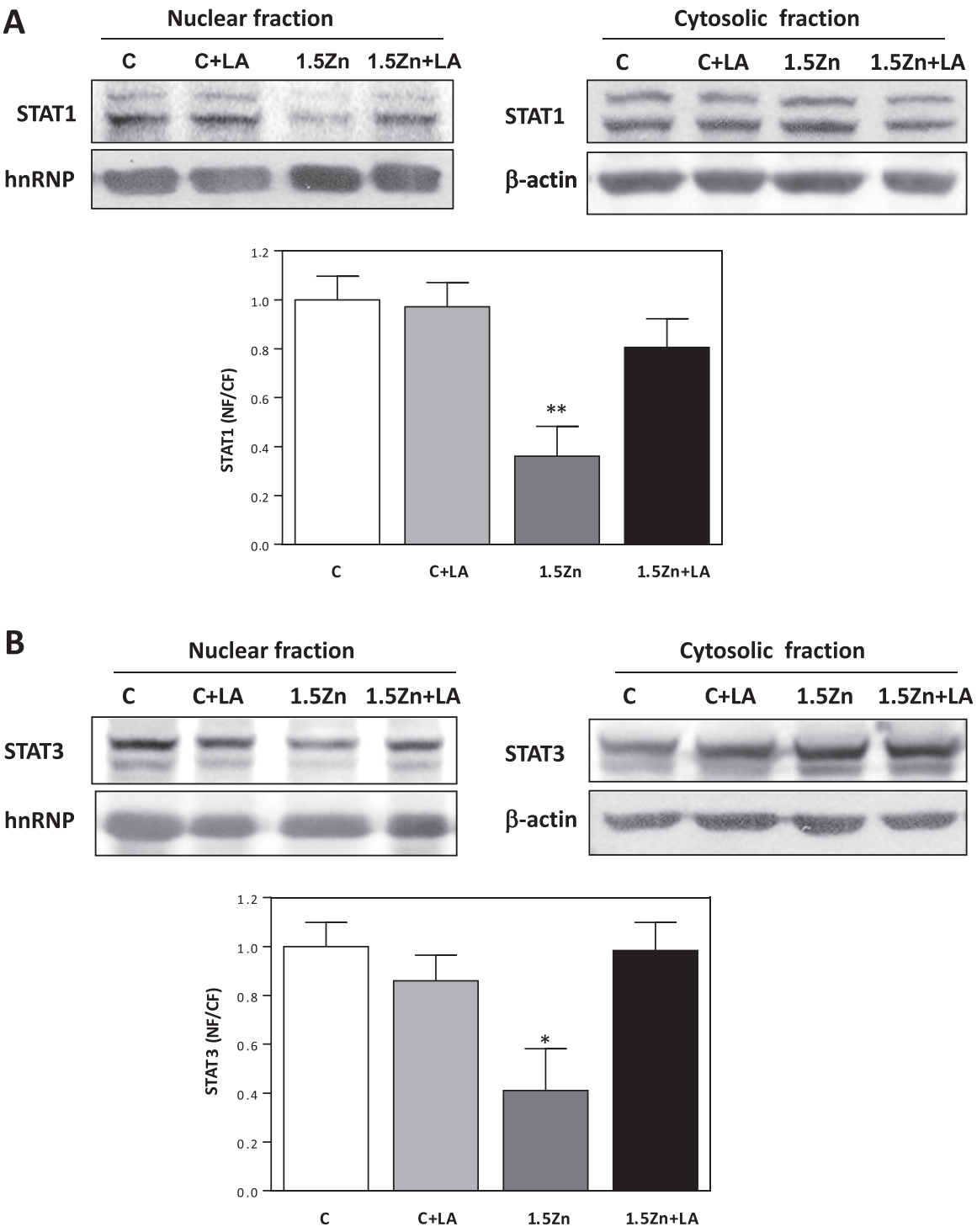

Fig. 7. α-Lipoic acid prevents zinc deficiency-induced impaired STAT1 and STAT3 nuclear import. Nuclear fraction and cytosolic fraction were isolated from IMR-32 cells incubated for 24 h in control (C), or zinc depleted (1.5Zn) medium with or without supplementation with 0.5mM α-lipoic acid (LA). Western blots for: (A) STAT1 and hnRNP as housekeeping protein in the nuclear fraction (top left), and STAT1 and β-actin as housekeeping protein in the cytosolic fraction (top right), and band quantification expressed as the ratio of total STAT1 nuclear/cytosolic (bottom); (B) STAT3 and hnRNP in the nuclear fraction (top left) and STAT3 and β-actin in the cytosolic fraction (top right), and band quantification expressed as the ratio total STAT3 nuclear/cytosolic fractions (bottom). Results were normalized to controls values, and shown as means ± S.E.M. of three independent experiments. *, ** Significantly different compared to C groups ($P < 0.05$ and $P < 0.01$, respectively, one-way ANOVA).

3.4. Zinc deficiency causes oxidative stress which is involved in the disruption of STAT1 and STAT3 nuclear translocation

4-hydroxynonenal (4-HNE) is a product of lipid oxidation that can diffuse and modify cellular components, including proteins. A potential condition of oxidative stress was assessed in E19 brains and IMR-32 cells by measuring 4-HNE-protein adducts. In the E19 brain, areas of stronger 4-HNE staining were identified by IHC to be mainly localized in the brain cortex **(**Fig. 6**A).** HNE-protein adducts were observed in the E19 MZD cortex, while they were mostly absent in controls. 4-HNE-protein adducts were evaluated by Western blot in IMR-32 cells incubated in control or 1.5Zn media for 24 h without or with supplementation with 0.5 mM LA. The 4-HNE staining of a band corresponding to a 50 kDa polypep-

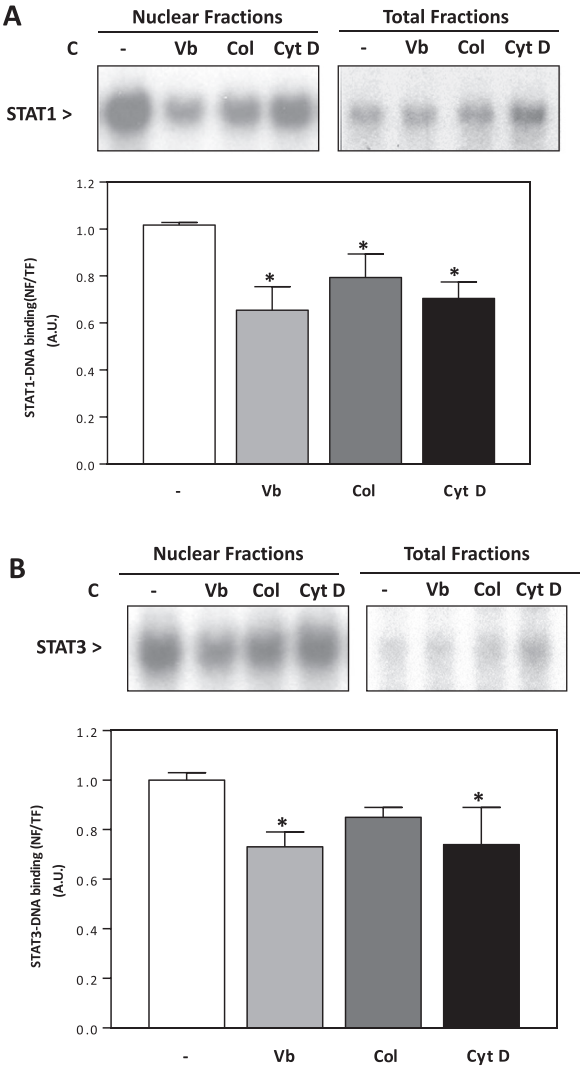

Fig. 8. STAT1 and STAT3 require a functional cytoskeleton for nuclear translocation in IMR-32 cells. Nuclear fractions and total fractions were prepared from IMR-32 cells incubated for 24 h in control medium (C) with or without the addition of 0.5 μM vinblastine (Vb), 0.5 μM colchicine (Col), or 0.5 μM cytochalasin D (Cyt D). (A) EMSA for STAT1 in nuclear and total fractions (top), and band quantifications (bottom). (B) EMSA for STAT3 in nuclear and total fractions (top), and band quantifications (bottom). Results were expressed as the ratio nuclear/total fractions of DNA binding (NF/TF) and normalized to their control levels. Results are shown as means ± S.E.M. of three independent experiments. *Significantly different compared to C without inhibitors ($P < 0.05$, one-way ANOVA).

tide in the Western blot was estimated to be 2.5-fold higher in 1.5Zn cells compared to controls, which was not observed upon co-incubation with 0.5 mM LA **(**Fig. 6**B).**

We previously observed that co-incubation of cells in zinc-depleted medium with LA prevented tubulin thiol oxidation and its impaired polymerization, restoring NF-κB nuclear transport [16]. Thus, we next investigated the effects of LA on STAT1 and STAT3 nuclear transport, by incubating IMR-32 cells in control or 1.5 Zn medium with or without supplementation with 0.5 mM LA. The total STAT1 and STAT3 protein levels in nuclear and cytosolic fractions were measured by Western blot. Ratios of nuclear/cytosolic STAT1 and STAT3 were significantly lower (64%, and 59%, respectively) in zinc deficient cells than in controls, and this was prevented by co-incubation with LA **(**Fig. 7**A and B)**.

3.5. Cytoskeleton disruptors impair STAT1 and STAT3 nuclear translocation

Based on the above findings, we investigated whether alterations to the cytoskeleton (i.e. tubulin and actin) polymerization could affect the nuclear translocation of STAT1 and STAT3 in IMR-32 cells. The actions of disrupting agents of tubulin (vinblastine and colchicine) and actin (cytochalasin D) polymerization on STAT1- and STAT3-DNA binding were investigated in nuclear fractions from IMR-32 cells incubated for 24 h with or without the inhibitors. The ratio nuclear/total STAT1-DNA binding was lower (36%, 22%, and 31%) in cells incubated with 0.5 μM vinblastine, colchicine and cytochalasin D, respectively, compared to controls **(**Fig. 8**A).** Similarly, vinblastine and cytochalasin D caused 27% and 26% reductions in the ratio nuclear/total STAT3-DNA binding, respectively, while no significant differences were observed for colchicine **(**Fig. 8**B)**.

3.6. LA prevents zinc deficiency-induced impaired tyrosine phosphorylation of STAT1 but not STAT3

We next investigated if oxidative stress could be involved in the zinc deficiency-mediated disruption of the upstream STAT1 and STAT3 tyrosine phosphorylation. IMR-32 cells were incubated for 24 h in control or 1.5Zn medium with or without 0.5 mM LA, and tyrosine phosphorylation was analyzed in total cell fractions by Western blot. The low STAT1 tyrosine-phosphorylation level observed in cells incubated in 1.5Zn medium was prevented by simultaneous incubation with LA **(**Fig. 9**A)**. However, LA failed to prevent the increase in STAT1 total protein expression caused by zinc deficiency **(**Fig. 9**A)**. LA also failed to prevent the decrease of tyrosine-phosphorylated STAT3 levels in zinc deficient cells **(**Fig. 9**B)**. As expected, zinc supplementation (15 μM) prevented the decrease of both STAT1 and STAT3 tyrosine phosphorylation in the zinc deficient cells (95 ± 9 and 109 ± 2% in 15Zn cells compared to control (100%), respectively (data not shown)). Zinc deficiency-induced increase in STAT1 serine phosphorylation, on the other hand, was not prevented by co-incubation with LA **(**Fig. 9**A)**.

4. Discussion

STAT1 and STAT3 play crucial roles in key developmental events; the deregulation caused by suboptimal gestational zinc nutrition could explain in part the deleterious effects on offspring brain development. This study provides novel evidence that zinc deficits both *in vivo* and *in vitro* disrupt STAT1 and STAT3 signaling pathways. This is evidenced by altered STAT1 and STAT3 phosphorylation patterns and decreased nuclear shuttling, which are in part due to zinc deficiency-induced oxidative stress.

Phosphorylation of STAT1 and STAT3 on serine residues [46] have multiple but still poorly defined functional consequences [47–49]. We observed that STAT1 serine phosphorylation levels were high, while STAT3 serine phosphorylation remained unchanged by zinc deficiency in both rat fetal brain and human IMR-32 cells. Zinc deficiency-induced oxidative stress leads to the activation of the redox-sensitive mitogen activated kinase p38 [9,50,51], which could explain the higher phosphorylation of STAT1 at Ser727 [52]. This was ruled out by the finding that, although LA inhibits zinc deficiency-induced p38 activation [50] it did not prevent the increase in STAT1 serine phosphorylation levels. Phosphorylation of STAT1 and STAT3 on tyrosine residues is involved in dimerization and nuclear translocation. STAT1 is phosphorylated in tyrosine by Jak2, which also phosphorylates microtubules facilitating the binding of STAT1 to tubulin for subsequent nuclear transport [53]. On the other hand, LA had no effect on the low STAT3 tyrosine phosphorylation levels in zinc deficient cells. A potential candidate that could explain STAT3 lower tyrosine levels is

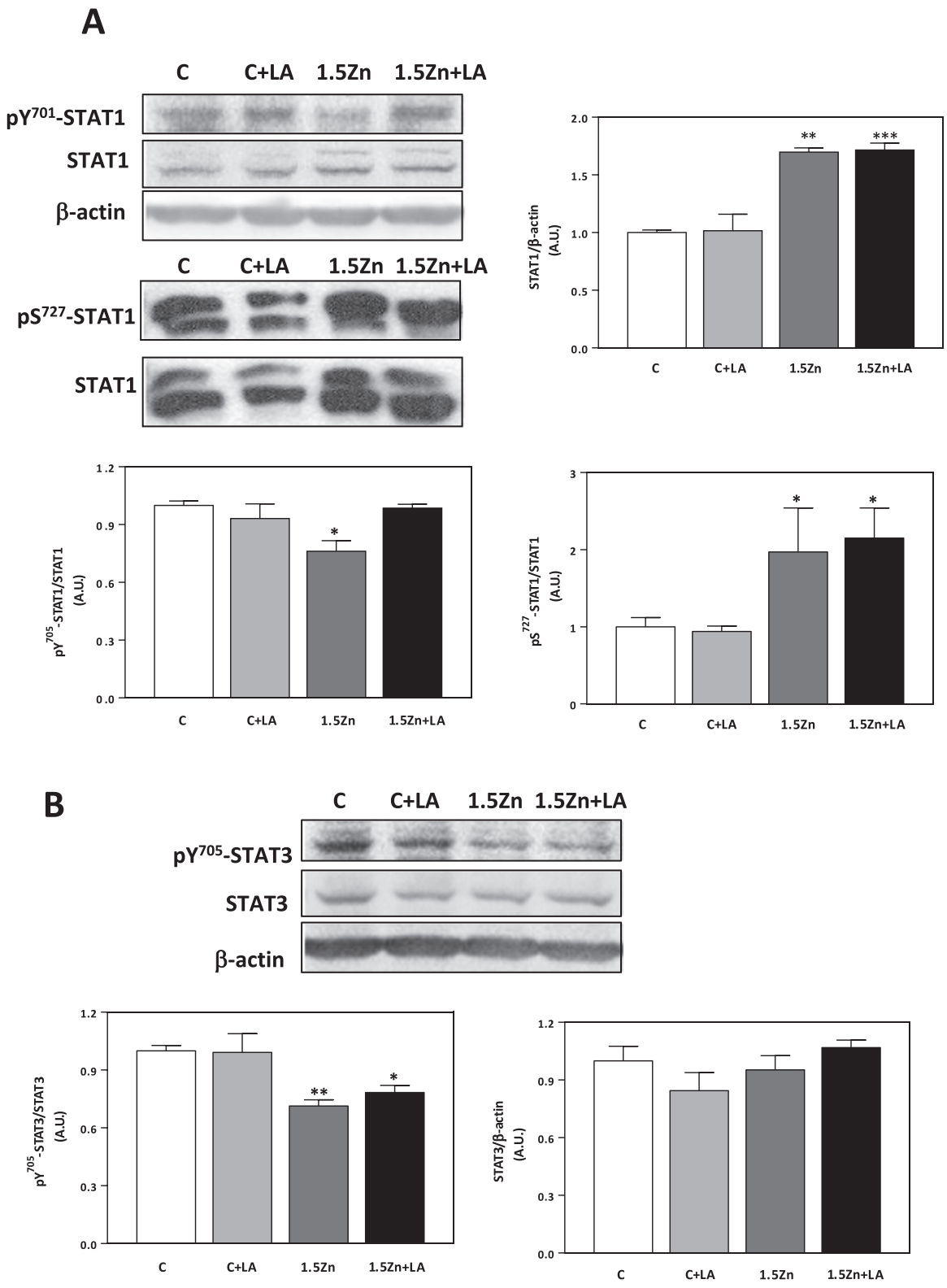

Fig. 9. α-Lipoic acid differentially affects STAT1 and STAT3 phosphorylation in zinc deficient IMR-32 cells. Total fractions were prepared from IMR-32 cells incubated for 24 h in control (C), or zinc deficient (1.5Zn) medium with or without supplementation with 0.5mM α-lipoic acid (LA). STAT1 and STAT3 content and phosphorylation were measured by Western blot. (A) Representative images for pY^{701}-STAT1, pS^{727}-STAT1, STAT1, and β-actin and their quantification expressed as pY^{701}-STAT1/STAT1, pS^{727}-STAT1/STAT1, and STAT1/β-actin (bottom). (B) Representative images for pY^{705}-STAT3, STAT3 and β-actin, and their quantification expressed as pY^{705}-STAT3/STAT3, and STAT3/β-actin. Results were normalized to control values and shown as means ± S.E.M. of four independent experiments. *, **, *** Significantly different compared to C groups ($P < 0.05$, $P < 0.01$, and $P < 0.001$, respectively, one-way ANOVA).

PTP1B, the STAT3 tyrosine phosphatase. PTP1B is regulated by both cell redox and zinc status [14]. Oxidation of a cysteine to sulfenylamide in the PTP1B catalytic domain inhibits the activity of the enzyme [54,55], while zinc per se inhibits PTP1B [56] which would lead to its activation in conditions of zinc deficits. This could explain the LA-insensitive decreased STAT3 tyrosine phosphorylation, and its recovery

upon zinc repletion. Further studies are needed to assess the participation of PTP1B, the differential responses of STAT1 and STAT3 phosphorylation to LA and their redox regulation in neuronal cells.

Tyrosine phosphorylation leads to STAT1 dimerization, which reveals a nuclear localization signal that is recognized by nuclear specific carriers (importins) for subsequent nuclear import [47–49]. While STAT3 tyrosine phosphorylation facilitates the dimer nuclear/cytoplasmic shuttling [57], STAT3 nuclear translocation can also occur independently of tyrosine phosphorylation [49,58]. LA restored both STAT1 and STAT3 nuclear transport in zinc deficient IMR-32 cells, but only prevented STAT1 decreased tyrosine phosphorylation. This suggests that under a condition of decreased zinc availability, the nuclear transport is the central event in the disruption of STAT1 and STAT3 activation and the subsequent STAT1- and STAT3-driven transactivating activity by zinc deficiency. As previously described [53,59–61], we observed that the cytoskeleton is required for STAT1 and STAT3 nuclear import in neuronal cells. Both in IMR-32 neuroblastoma cells and in fetal brain, zinc deficiency alters tubulin polymerization dynamics via oxidative stress-induced oxidation of tubulin thiols [16,18]. We previously showed that alterations in tubulin polymerization underlies zinc deficiency-associated impaired nuclear translocation of transcription factors NF-κB and NFAT in fetal rat brain, rat cortical neurons, differentiated PC12 cells and proliferating IMR-32 cells [16–18]. In fact, reduction of tubulin disulfides upon treatment with LA restored tubulin assembly and NF-κB nuclear translocation in zinc deficient IMR-32 cells [16]. In this study, we observed that zinc deficiency is associated with the accumulation of 4-HNE adducts in E19 rat brain and IMR-32 cells. 4-HNE has been shown to form adducts with tubulin involving Lys residues, which leads to the formation of aggregates and to impaired polymerization [62]. Findings that: i) under identical experimental conditions to those used in the current work LA prevented zinc deficiency induced tubulin oxidation and altered polymerization [16], ii) LA prevented zinc deficiency-associated decrease in nuclear STAT1 and STAT3, iii) the requirement of microtubules for STAT1 and STAT3 nuclear transport [53,59–61]; suggest that tubulin oxidation contributes to the impaired nuclear import of STAT1 and STAT3 under conditions of zinc deficits. Current results also suggest the involvement of tubulin and actin in STAT1 and STAT3 nuclear transport. Recent observations of lower STAT3 binding to both tubulin and actin in the zinc deficient E19 brain (unpublished results) grant future research on the role of both actin and tubulin redox status on STAT3 and STAT1 modulation under conditions of decreased zinc availability.

In summary, a low zinc availability affected STAT1 and STAT3 modulation in both E19 rat brain and human neuroblastoma IMR-32 cells. Zinc deficiency caused oxidative modification of proteins, altered patterns of STAT1 and STAT3 phosphorylation, impaired nuclear translocation, DNA binding, and trans-activating activity. The data presented herein suggest a role for zinc deficiency-induced oxidative stress on the impaired tyrosine phosphorylation and nuclear shuttling of STAT1 and STAT3. The latter, together with the previously shown impaired nuclear transport of transcription factors NFAT and NF-κB, stresses the relevance of tubulin oxidation and altered cytoskeleton dynamics as central events in zinc deficiency-associated pathophysiology. Given the major and different roles that STAT1 and STAT3 play in the nervous system, their impaired modulation could in part explain the deleterious effects of gestational marginal zinc deficiency on early brain development.

Acknowledgements and conflict of interest disclosure

This work was supported by Grants from NIFA-USDA (CA-D*-XXX-7244-H), and the PackerWentz Endowment. S. Supasai was a fellow from the Thailand Government. The authors have no conflicting interests to declare.

Appendix A. Supporting information

Supplementary data associated with this article can be found in the online version at doi:10.1016/j.redox.2016.12.027.

References

[1] C.J. Frederickson, J.Y. Koh, A.I. Bush, The neurobiology of zinc in health and disease, Nat. Rev. Neurosci. 6 (2005) 449–462.
[2] L.E. Caulfield, N. Zavaleta, A.H. Shankar, M. Merialdi, Potential contribution of maternal zinc supplementation during pregnancy to maternal and child survival, Am. J. Clin. Nutr. 68 (1998) 499S–508S.
[3] L.A. Scheplyagina, Impact of the mother's zinc deficiency on the woman's and newborn's health status, J. Trace Elem. Med Biol. 19 (2005) 29–35.
[4] C.A. Swanson, J.C. King, Zinc and pregnancy outcome, Am. J. Clin. Nutr. 46 (1987) 763–771.
[5] L. Hubbs-Tait, T.S. Kennedy, E.A. Droke, D.M. Belanger, J.R. Parker, Zinc, iron, and lead: relations to head start children's cognitive scores and teachers' ratings of behavior, J. Am. Diet. Assoc. 107 (2007) 128–133.
[6] R.L. Goldenberg, T. Tamura, Y. Neggers, R.L. Copper, K.E. Johnston, M.B. DuBard, et al., The effect of zinc supplementation on pregnancy outcome, JAMA 274 (1995) 463–468.
[7] M.A. Jankowski, J.Y. Uriu-Hare, R.B. Rucker, J.M. Rogers, C.L. Keen, Maternal zinc deficiency, but not copper deficiency or diabetes, results in increased embryonic cell death in the rat: implications for mechanisms underlying abnormal development, Teratology 51 (1995) 85–93.
[8] X. Yu, L. Jin, X. Zhang, X. Yu, Effects of maternal mild zinc deficiency and zinc supplementation in offspring on spatial memory and hippocampal neuronal ultrastructural changes, Nutrition 29 (2013) 457–461.
[9] L. Aimo, G.G. Mackenzie, A.H. Keenan, P.I. Oteiza, Gestational zinc deficiency affects the regulation of transcription factors AP-1, NF-kappaB and NFAT in fetal brain, J. Nutr. Biochem. 21 (2010) 1069–1075.
[10] W. Chowanadisai, S.L. Kelleher, B. Lonnerdal, Maternal zinc deficiency reduces NMDA receptor expression in neonatal rat brain, which persists into early adulthood, J. Neurochem. 94 (2005) 510–519.
[11] E.S. Halas, M.J. Eberhardt, M.A. Diers, H.H. Sandstead, Learning and memory impairment in adult rats due to severe zinc deficiency during lactation, Physiol. Behav. 30 (1983) 371–381.
[12] E.S. Halas, M.D. Heinrich, H.H. Sandstead, Long term memory deficits in adult rats due to postnatal malnutrition, Physiol. Behav. 22 (1979) 991–997.
[13] E.S. Halas, C.D. Hunt, M.J. Eberhardt, Learning and memory disabilities in young adult rats from mildly zinc deficient dams, Physiol. Behav. 37 (1986) 451–458.
[14] P.I. Oteiza, Zinc and the modulation of redox homeostasis, Free Radic. Biol. Med. 53 (2012) 1748–1759.
[15] L. Aimo, G.N. Cherr, P.I. Oteiza, Low extracellular zinc increases neuronal oxidant production through nadph oxidase and nitric oxide synthase activation, Free Radic. Biol. Med. 48 (2010) 1577–1587.
[16] G.G. Mackenzie, G.A. Salvador, C. Romero, C.L. Keen, P.I. Oteiza, A deficit in zinc availability can cause alterations in tubulin thiol redox status in cultured neurons and in the developing fetal rat brain, Free Radic. Biol. Med. 51 (2011) 480–489.
[17] G.G. Mackenzie, P.I. Oteiza, Zinc and the cytoskeleton in the neuronal modulation of transcription factor NFAT, J. Cell Physiol. 210 (2007) 246–256.
[18] G.G. Mackenzie, C.L. Keen, P.I. Oteiza, Microtubules are required for NF-kappaB nuclear translocation in neuroblastoma IMR-32 cells: modulation by zinc, J. Neurochem. 99 (2006) 402–415.
[19] G.G. Mackenzie, M.P. Zago, C.L. Keen, P.I. Oteiza, Low intracellular zinc impairs the translocation of activated NF-kappa B to the nuclei in human neuroblastoma IMR-32 cells, J. Biol. Chem. 277 (2002) 34610–34617.
[20] H.S. Kim, M.S. Lee, STAT1 as a key modulator of cell death, Cell. Signal. 19 (2007) 454–465.
[21] J. Bromberg, J.E. Darnell Jr., The role of STATs in transcriptional control and their impact on cellular function, Oncogene 19 (2000) 2468–2473.
[22] A.L. Mui, The role of STATs in proliferation, differentiation, and apoptosis, Cell Mol. Life Sci. 55 (1999) 1547–1558.
[23] M.A. Meraz, J.M. White, K.C. Sheehan, E.A. Bach, S.J. Rodig, A.S. Dighe, et al., Targeted disruption of the Stat1 gene in mice reveals unexpected physiologic specificity in the JAK-STAT signaling pathway, Cell 84 (1996) 431–442.
[24] J.E. Durbin, A. Fernandez-Sesma, C.K. Lee, T.D. Rao, A.B. Frey, T.M. Moran, et al., Type I IFN modulates innate and specific antiviral immunity, J. Immunol. 164 (2000) 4220–4228.
[25] A.J. Filiano, Y. Xu, N.J. Tustison, R.L. Marsh, W. Baker, I. Smirnov, et al., Unexpected role of interferon-gamma in regulating neuronal connectivity and social behaviour, Nature 535 (2016) 425–429.
[26] A. Bonni, Y. Sun, M. Nadal-Vicens, A. Bhatt, D.A. Frank, I. Rozovsky, et al., Regulation of gliogenesis in the central nervous system by the JAK-STAT signaling pathway, Science 278 (1997) 477–483.
[27] A.M. Planas, C. Justicia, I. Ferrer, Stat1 in developing and adult rat brain. Induction after transient focal ischemia, Neuroreport 8 (1997) 1359–1362.
[28] W. Lin, A. Kemper, K.D. McCarthy, P. Pytel, J.P. Wang, I.L. Campbell, et al., Interferon-gamma induced medulloblastoma in the developing cerebellum, J. Neurosci. 24 (2004) 10074–10083.
[29] S. Dziennis, N.J. Alkayed, Role of signal transducer and activator of transcription 3 in neuronal survival and regeneration, Rev. Neurosci. 19 (2008) 341–361.
[30] F.D. Miller, A.S. Gauthier, Timing is everything: making neurons versus glia in the

developing cortex, Neuron 54 (2007) 357–369.
[31] K. Takeda, K. Noguchi, W. Shi, T. Tanaka, M. Matsumoto, N. Yoshida, et al., Targeted disruption of the mouse Stat3 gene leads to early embryonic lethality, Proc. Natl. Acad. Sci. USA 94 (1997) 3801–3804.
[32] M.M. Sherry, A. Reeves, J.K. Wu, B.H. Cochran, STAT3 is required for proliferation and maintenance of multipotency in glioblastoma stem cells, Stem Cells 27 (2009) 2383–2392.
[33] J. Vernerey, M. Macchi, K. Magalon, M. Cayre, P. Durbec, Ciliary neurotrophic factor controls progenitor migration during remyelination in the adult rodent brain, J. Neurosci. 33 (2013) 3240–3250.
[34] H. Asano, M. Aonuma, T. Sanosaka, J. Kohyama, M. Namihira, K. Nakashima, Astrocyte differentiation of neural precursor cells is enhanced by retinoic acid through a change in epigenetic modification, Stem Cells 27 (2009) 2744–2752.
[35] S.S. Zhang, M.G. Liu, A. Kano, C. Zhang, X.Y. Fu, C.J. Barnstable, STAT3 activation in response to growth factors or cytokines participates in retina precursor proliferation, Exp. Eye Res. 81 (2005) 103–115.
[36] V. Sriuranpong, J.I. Park, P. Amornphimoltham, V. Patel, B.D. Nelkin, J.S. Gutkind, Epidermal growth factor receptor-independent constitutive activation of STAT3 in head and neck squamous cell carcinoma is mediated by the autocrine/paracrine stimulation of the interleukin 6/gp130 cytokine system, Cancer Res. 63 (2003) 2948–2956.
[37] K. Szczepanek, E.J. Lesnefsky, A.C. Larner, Multi-tasking: nuclear transcription factors with novel roles in the mitochondria, Trends Cell Biol. 22 (2012) 429–437.
[38] M.J. Waters, A.J. Brooks, JAK2 activation by growth hormone and other cytokines, Biochem. J. 466 (2015) 1–11.
[39] L.A. O'Sullivan, C. Liongue, R.S. Lewis, S.E. Stephenson, A.C. Ward, Cytokine receptor signaling through the Jak-Stat-Socs pathway in disease, Mol. Immunol. 44 (2007) 2497–2506.
[40] D.E. Levy, J.E. Darnell Jr., Stats: transcriptional control and biological impact, Nat. Rev. Mol. Cell Biol. 3 (2002) 651–662.
[41] C.L. Keen, J.M. Peters, L.S. Hurley, The effect of valproic acid on 65Zn distribution in the pregnant rat, J. Nutr. 119 (1989) 607–611.
[42] P.I. Oteiza, M.S. Clegg, M.P. Zago, C.L. Keen, Zinc deficiency induces oxidative stress and AP-1 activation in 3T3 cells, Free Radic. Biol. Med. 28 (2000) 1091–1099.
[43] J.D. Dignam, R.M. Lebovitz, R.G. Roeder, Accurate transcription initiation by RNA polymerase II in a soluble extract from isolated mammalian nuclei, Nucleic Acids Res. 11 (1983) 1475–1489.
[44] L. Osborn, S. Kunkel, G.J. Nabel, Tumor necrosis factor alpha and interleukin 1 stimulate the human immunodeficiency virus enhancer by activation of the nuclear factor kappa B, Proc. Natl. Acad. Sci. USA 86 (1989) 2336–2340.
[45] M.M. Bradford, A rapid and sensitive method for the quantitation of microgram quantities of protein utilizing the principle of protein-dye binding, Anal. Biochem. 72 (1976) 248–254.
[46] T. Decker, P. Kovarik, Serine phosphorylation of STATs, Oncogene 19 (2000) 2628–2637.
[47] K.M. McBride, N.C. Reich, The ins and outs of STAT1 nuclear transport, Sci. STKE. 2003 (2003) Re13.
[48] N.C. Reich, STAT dynamics, Cytokine Growth Factor Rev. 18 (2007) 511–518.
[49] N.C. Reich, STATs get their move on, Jakstat 2 (2013) e27080.
[50] G.G. Mackenzie, M.P. Zago, A.G. Erlejman, L. Aimo, C.L. Keen, P.I. Oteiza, Alpha-Lipoic acid and N-acetyl cysteine prevent zinc deficiency-induced activation of NF-kappaB and AP-1 transcription factors in human neuroblastoma IMR-32 cells, Free Radic. Res. 40 (2006) 75–84.
[51] M.P. Zago, G.G. Mackenzie, A.M. Adamo, C.L. Keen, P.I. Oteiza, Differential modulation of MAP kinases by zinc deficiency in IMR-32 cells: role of H(2)O(2), Antioxid. Redox Signal. 7 (2005) 1773–1782.
[52] P. Kovarik, D. Stoiber, P.A. Eyers, R. Menghini, A. Neininger, M. Gaestel, et al., Stress-induced phosphorylation of STAT1 at Ser727 requires p38 mitogen-activated protein kinase whereas IFN-gamma uses a different signaling pathway, Proc. Natl. Acad. Sci. USA 96 (1999) 13956–13961.
[53] X. Ma, P.P. Sayeski, Identification of tubulin as a substrate of Jak2 tyrosine kinase and its role in Jak2-dependent signaling, Biochemistry 46 (2007) 7153–7162.
[54] Z.Y. Zhang, Y. Wang, J.E. Dixon, Dissecting the catalytic mechanism of protein-tyrosine phosphatases, Proc. Natl. Acad. Sci. USA 91 (1994) 1624–1627.
[55] A. Salmeen, J.N. Andersen, M.P. Myers, T.C. Meng, J.A. Hinks, N.K. Tonks, et al., Redox regulation of protein tyrosine phosphatase 1B involves a sulphenyl-amide intermediate, Nature 423 (2003) 769–773.
[56] H. Haase, W. Maret, Intracellular zinc fluctuations modulate protein tyrosine phosphatase activity in insulin/insulin-like growth factor-1 signaling, Exp. Cell Res. 291 (2003) 289–298.
[57] A. Herrmann, U. Sommer, A.L. Pranada, B. Giese, A. Kuster, S. Haan, et al., STAT3 is enriched in nuclear bodies, J. Cell Sci. 117 (2004) 339–349.
[58] L. Liu, K.M. McBride, N.C. Reich, STAT3 nuclear import is independent of tyrosine phosphorylation and mediated by importin-alpha3, Proc. Natl. Acad. Sci. USA 102 (2005) 8150–8155.
[59] S.R. Walker, M. Chaudhury, E.A. Nelson, D.A. Frank, Microtubule-targeted chemotherapeutic agents inhibit signal transducer and activator of transcription 3 (STAT3) signaling, Mol. Pharmacol. 78 (2010) 903–908.
[60] S.R. Walker, M. Chaudhury, D.A. Frank, STAT3 inhibition by, Mol. Cell Pharmacol. 3 (2011) 13–19.
[61] G.W. Moseley, X. Lahaye, D.M. Roth, S. Oksayan, R.P. Filmer, C.L. Rowe, et al., Dual modes of rabies P-protein association with microtubules: a novel strategy to suppress the antiviral response, J. Cell Sci. 122 (2009) 3652–3662.
[62] B.J. Stewart, J.A. Doorn, D.R. Petersen, Residue-specific adduction of tubulin by 4-hydroxynonenal and 4-oxononenal causes cross-linking and inhibits polymerization, Chem. Res. Toxicol. 20 (2007) 1111–1119.